Joule

CellPress
OPEN ACCESS

Report

Large-area organic photovoltaic modules with 14.5% certified world record efficiency

Robin Basu, Fabian Gumpert, Jan Lohbreier, ..., Christoph J. Brabec, Hans-Joachim Egelhaaf, Andreas Distler

andreas.distler@fau.de

Highlights

New world record efficiency for large-area organic photovoltaic (OPV) modules

14.5% certified power conversion efficiency on total module area, 15.0% on active area

Barely any performance loss upon upscaling from 4-mm^2 cells to >200-cm^2 modules

Industry-relevant processing in ambient air from non-halogenated solvents

A new certified world record efficiency for large-area organic photovoltaic (OPV) modules is demonstrated, namely 14.5% on the total module area (15.0% on active area). This achievement is enabled by finite element method (FEM) computer simulations used to optimize the coating homogeneity and the solar module layout. Barely any performance loss is observed when scaling 4-mm^2 cells up to >200-cm^2 modules. All functional layers are processed in ambient air from non-halogenated solvents.

Basu et al., Joule 8, 970–978
April 17, 2024
https://doi.org/10.1016/j.joule.2024.02.016

CellPress OPEN ACCESS

Joule

Report

Large-area organic photovoltaic modules with 14.5% certified world record efficiency

Robin Basu,[1] Fabian Gumpert,[2] Jan Lohbreier,[2] Pierre-Olivier Morin,[3] Varun Vohra,[3] Yang Liu,[4] Yinhua Zhou,[4] Christoph J. Brabec,[1,5] Hans-Joachim Egelhaaf,[1,5] and Andreas Distler[1,6,*]

SUMMARY

Organic photovoltaics (OPVs) have experienced a significant increase in power conversion efficiency (PCE) recently, now approaching 20% on small-cell level. Since the efficiencies on the module level are still substantially lower, focused upscaling research is necessary to reduce the gap between cells and modules. In this work, we present the upscaling of PM6:Y6-C12:PC_{61}BM-based devices, processed in ambient air from non-halogenated solvents, from small-area cells to large-area modules with barely any performance loss. Supported by computational fluid dynamics simulations, an accelerated blade coating process that enables homogeneous coatings with <5% thickness deviation over 200 cm^2 is developed. Additional finite element method simulations are used to optimize the module layout and minimize the inevitable losses caused by electrode resistances and inactive interconnect areas to 1.9% and 3.5%, respectively. Finally, a 204-cm^2 OPV module with a certified PCE of 14.5% (15.0% on active area) is fabricated, which constitutes the new world record.

CONTEXT & SCALE

Organic photovoltaics (OPVs) are a promising emerging PV technology with unique benefits, such as light weight, flexibility, transparency, tunable spectral absorbance, and a low-cost/-energy production process. With a power conversion efficiency (PCE) of close to 20% on small-cell level, OPVs are rapidly approaching the performance of conventional PV technologies. However, such high PCE values have not been able to be transferred to larger areas and the module level yet, which hinders the successful commercialization of the technology and impedes its entry into promising markets, such as building integration, aerospace applications, or agrivoltaics.

This work presents cutting-edge upscaling research on OPVs that aims at closing the efficiency gap between high-performance cells and modules. Utilizing computer simulations, the layout and manufacturing process of large-area OPV modules is optimized. Through this, a new certified world record efficiency for OPV modules of 14.5% is achieved and demonstrated.

INTRODUCTION

During the last few years, the development of new absorber materials has led to a significant boost in power conversion efficiencies (PCEs) of organic solar cells, now approaching 20% on small-cell level.[1] Thus, organic photovoltaics (OPVs) are finally approaching the performance of conventional photovoltaic (PV) technologies. In order to eventually experience a breakthrough on the market, these high PCE values first need to be scaled to large areas and the module level, though. To this end, upscaling research aims at reducing the PCE gap between small cells (few mm^2) and large modules (>200 cm^2) to the minimum.

For cell-to-module upscaling, the crucial challenges are (1) to minimize the resistive losses (e.g., caused by the transparent electrode or the interconnects [ICs]), (2) the reduction of inactive areas within the total module area (i.e., maximizing the geometric fill factor [GFF]), and (3) the large-area deposition of all layers without defects and with high homogeneity.[2] Moreover, it is important to evaluate and select material systems, architectures, and processes that can easily be transferred to a larger scale. This implies a solution-processed layer stack, materials well-soluble in non-halogenated solvents, utilization of meniscus-guided coating techniques, and processing in ambient air.[3–5]

Current state-of-the-art OPV "minimodules" with active areas of typically 5–40 mm^2 reach 13%–15% PCE,[6–10] with the best modules even having values close to the current record PCE of 1-cm^2 cells (15.8%).[11] However, since upscaling becomes increasingly complex with increasing device area, hardly any high-performance OPV modules in the "sub-module" category (i.e., >200 cm^2) have been reported yet.[12]

To reach high PCE values on the *active* module area, a homogeneous large-area coating is the most challenging task for large-area OPV modules. However, a "real" module PCE always refers to the *total* module area (as reported by certified measurements), which also includes the inactive areas that are used for cell interconnection. The latter requires additional optimizations regarding the module layout, e.g., strategies to maximize the GFF.[13,14] Both aspects are highlighted in this work.

For this work, the active material system PM6:Y6-C12:PC_{61}BM (see experimental procedures) is chosen, because (1) PM6 provides very high performance and exceptional reproducibility on large areas and is thus the currently most-used polymer for high-efficiency OPV modules[2]; (2) in combination with PM6, the non-fullerene acceptor Y6-C12 provides a similar high efficiency as Y6 but makes the system well-processable from non-halogenated solvents due to its longer side chains[15,16]; and (3) the addition of small amounts of fullerenes has been shown to improve device performance by increasing phase purities and charge mobilities inside the active layer.[17]

Herein, we upscale PM6:Y6-C12:PC_{61}BM coated from o-xylene in ambient air by using a solution-processed stack (active layer and both charge transport layers). The respective blade coating processes and the module layout are optimized by means of computational fluid dynamics (CFD) and electrical finite element method (FEM) simulations, respectively, to maximize performance. Finally, a 204-cm^2 module with a new certified world record PCE of 14.5% is demonstrated.

RESULTS AND DISCUSSION

For the performance of OPV cells, the thicknesses of all functional layers (especially the photoactive layer) play a decisive role. Hence, for modules, the targeted thicknesses of all layers need to be met as precisely as possible over the whole device area. While regular blade coating is the most common and material-saving processing technique for OPV modules, it has the drawback that coating over larger distances (>5 cm) leads to a thickness gradient in the deposited film.[9] The reason for this phenomenon is that the film thickness decreases with decreasing ink volume inside the gap between substrate and applicator, as described by Gumpert et al.,[18] which naturally happens during coating, since part of the ink is deposited onto the substrate to form the film. Another correlation that has been observed in doctor-bladed films is that the film thickness increases with the coating speed. Consequently, the steadily decreasing ink volume can be compensated by a gradually increased velocity to maintain the same film thickness over long distances. Such an "accelerated blade coating" approach was first reported by Nickel et al.[19] and further utilized for the mentioned purpose of large-area OPV coatings by Tsai et al.[20] However, the correlation of film thickness, ink volume, and coating speed is complex (i.e., there is no simple acceleration factor) and specific to the blade geometry and the ink properties.

Therefore, we developed a CFD simulation model that is able to predict the film thickness based on a given setup geometry, ink viscosity, and ink surface energy (details are reported in Gumpert et al.[18] and Gumpert et al.[21]). Based on these

[1]Friedrich-Alexander-Universität Erlangen-Nürnberg, Faculty of Engineering, Department of Material Science, Materials for Electronics and Energy Technology (i-MEET), Martensstraße 7, 91058 Erlangen, Germany

[2]Nuremberg Institute of Technology, Faculty of Applied Mathematics, Physics and Humanities, Group Computational Physics for Green Energy, Keßlerplatz 12, 90489 Nuremberg, Germany

[3]Brilliant Matters, 237 Rue de Liverpool, Saint-Augustin-de-Desmaures, QC G3A 2C8, Canada

[4]Wuhan National Laboratory for Optoelectronics, Huazhong University of Science and Technology, Wuhan 430074, China

[5]Forschungszentrum Jülich GmbH, Helmholtz Institute Erlangen-Nürnberg for Renewable Energy (HI-ERN), Immerwahrstraße 2, 91058 Erlangen, Germany

[6]Lead contact

*Correspondence: andreas.distler@fau.de

https://doi.org/10.1016/j.joule.2024.02.016

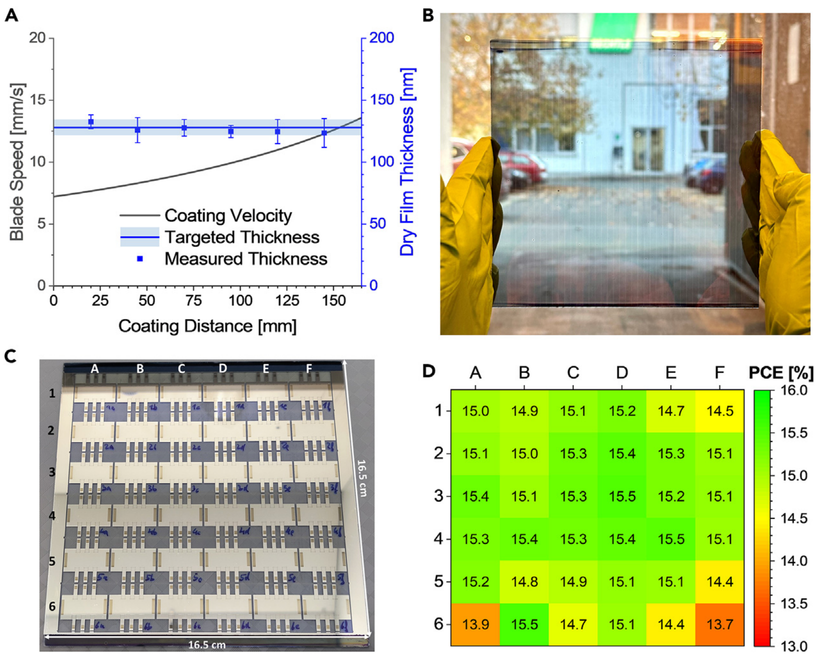

Figure 1. Coating homogeneity optimization and evaluation

(A) Velocity profile of the accelerated blade coating of PM6:Y6-C12:$PC_{61}BM$ (black line) over a distance of 165 mm, targeted thickness value ±5% (blue line and light blue area), and resulting thicknesses measured at 36 (6x6) different points (blue data points and error bars) of a 165 × 165 mm glass/ITO substrate.

(B) Photograph of the respective film as part of a half-finished solar module that is already P2 laser-patterned (i.e., the active layer is already partially removed again, as can be seen from the thin vertical transparent lines).

(C) Photograph of a 165 × 165 mm substrate comprising 216 individual solar cells.

(D) Respective power conversion efficiency (PCE) of such a set of solar cells (averaged in groups of six) with the layer stack glass/ITO/ZnO/PM6:Y6-C12:$PC_{61}BM$/PEDOT-F/Ag.

simulations, we obtained a specific acceleration profile for all inks used in this work, namely sol-gel zinc oxide (ZnO) as electron transport material, PM6:Y6-C12:$PC_{61}BM$ as active material, and PEDOT:F as hole-transport material (see Figure S1 in the supplemental information).

The velocity profile of the active layer coating over a distance of 165 mm is shown in Figure 1A as a black line together with the targeted optimized thickness of 128 nm ± 5% (blue line and light blue area, respectively). The photograph (Figure 1B) shows the result of such an accelerated coating of PM6:Y6-C12:$PC_{61}BM$ in o-xylene on a 165 × 165 mm glass/indium tin oxide (ITO) substrate and demonstrates the excellent homogeneity of the film. The respective film thickness is measured at six different vertical and horizontal positions on the substrate (see blue data points and error bars, respectively, in Figure 1A). A deviation of less than 5% from the targeted thickness is observed over the whole area.

Apart from the film thickness distribution over the substrate area, we also wanted to evaluate the effective PCE of the final layer stack at different positions in order to be able to detect potential areas of lower performance, relate them to a specific layer, and finally optimize the respective coating to maximize the average performance over the whole substrate. To this end, we created a layout, which comprises 216 individual small (4 mm^2) solar cells spread over one 165 × 165 mm substrate (see

Figure 1C). The PCEs of such set of solar cells with the layer stack glass/ITO/ZnO/PM6:Y6-C12:PC_{61}BM/PEDOT-F/Ag, the electron transport layer (ETL), active layer (AL), and hole transport layer (HTL), all being blade-coated from non-halogenated solvents in ambient air, are plotted in Figure 1D as a heatmap. The respective heatmaps of short-circuit current (J_{sc}), open-circuit voltage (V_{oc}), and fill factor (FF) can be found in the supplemental information (Figure S2). In general, we find a very homogeneous PCE distribution over the whole substrate area. Only slightly lower values are observed in three of the four corners, which in fact coincided with our optical inspection of the ETL coating, showing a rough (i.e., light-scattering) surface at these positions. We were able to relate this to the preceding substrate cleaning procedure (wiping with a microfiber tissue) and changed it accordingly (see experimental procedures) to overcome this issue.

In order to ensure the stability of the device stack, selected cells were measured for half an hour under constant illumination, which equals the typical time frame of a certified measurement, and stable performance is confirmed (Figure S3).

Since the PCE of a PV module should always be reported with respect to its full area, as it is done in certified measurements, this includes inactive module areas that do not directly contribute to the power conversion. These so-called "IC areas" are necessary to separate the individual sub-cells of a module and connect them electrically in series. The ratio of active module area (i.e., excluding ICs) and total module area (i.e., including ICs) is called GFF. The more cells (and thus ICs) a module has, the lower the GFF and consequently also the PCE of the PV module. On the other hand, the wider the active area of each individual sub-cell is, the higher the resistance losses caused by the electrodes, especially the transparent front electrode (e.g., ITO).[22] Consequently, there is a trade-off between these two aspects, and for a given total module width, there is one optimum number of cells the module should be divided into, in order to maximize the module's PCE. This optimum strongly depends on factors like the ITO sheet resistance, the current density provided by the solar cell stack, and the width of one individual IC.

In order to find this optimum for any desired module geometry and used layer stack, we developed an FEM simulation model that computes the module current-voltage (I-V) curve based on an input I-V curve taken from small-cell measurements, for which resistance losses are negligible, and other physical and geometrical input parameters. The model, which is an extended version of the one previously published by Lucera et al.,[23] varies the number of sub-cells on a given area, simulates the resulting potential distributions and current flows, and outputs the PCE of the total module for each variation.

This procedure is performed for a predefined total module area of 143 × 143 mm, an IC width of 135 μm consisting of P1+P2+P3 (see microscope image in Figure S4), an ITO sheet resistance of 11 Ω/sq, and an input I-V curve of a 4-mm^2 solar cell with a PCE of 15.0% taken from the above-described cell experiment. The model, including the whole set of input parameters and detailed results, can be found in the supplemental information (Figures S5 and S6; Table S1). Figure 2A summarizes the simulated PCE losses of the module as a function of sub-cell number (top axis) and the respective active sub-cell width (bottom axis). The total PCE losses (blue = $1 - PCE_{total}/PCE_{input}$) are the combination of the resistance losses (red = $1 - PCE_{active}/PCE_{input}$) and GFF losses (black = $1 - PCE_{active}/PCE_{total}$). The lowest overall losses, namely 5.33%, are observed for a module with 38 sub-cells of 3.63 mm active width, leading to a total module PCE of 14.20%. The resistance losses and GFF losses in this case amount to 1.91% and 3.49%, respectively.

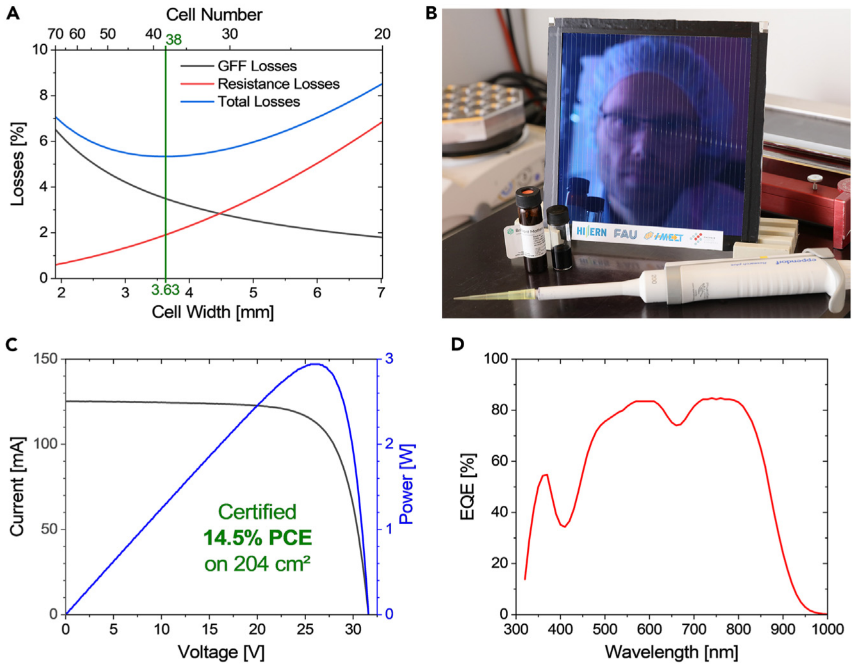

Figure 2. Solar module layout optimization and certified world record module

(A) Simulated PCE loss analysis of a 143 × 143 mm module based on PM6:Y6-C12:$PC_{61}BM$ as a function of sub-cell number.

(B) Photograph of such a module with 38 sub-cells.

(C) Certified current-voltage and power-voltage measurements performed by Fraunhofer ISE (Freiburg, Germany) on this module.

(D) Respective certified external quantum efficiency (EQE) curve, measured on the total module area (204.11 cm^2), and recalculated to the active area of one sub-cell (5.18 cm^2).

Based on this optimized layout and the above-described accelerated coating processes, an OPV module with 204 cm^2 is manufactured and measured under standard testing conditions (25°C module temperature, 1,000 W/m^2 AM1.5G irradiation). A photograph of this module is shown in Figure 2B, and the results of our in-house measurements are summarized in Table 1. Having a PCE of 14.6%, this OPV submodule provides an electrical power output of 3 W in its maximum power point (MPP) under one sun illumination. Considering its GFF of 96.5%, a value that can be achieved with high reproducibility (see Figure S4), the module possesses an outstanding PCE of 15.1% with respect to its active area. Remarkably, the module has an exceptionally high FF of 76.0%, which is as high as that of the respective 4-mm^2 cells. Moreover, we want to highlight at this point again that the active layer as well as both charge extraction layers of the module are blade-coated from non-halogenated solvents in ambient air.

Finally, this module was sent to the Fraunhofer Institute for Solar Energy Systems ISE in Freiburg/Germany for a certified measurement. The results of this measurement are also summarized in Table 1, and the respective current/power-voltage characteristics and the external quantum efficiency (EQE) curve are plotted in Figures 2C and 2D, respectively. The certificates are provided as supplemental information. All certified key parameters are found to be very similar (±2%) to our in-house measurement. Most importantly, a PCE of 14.46% on 204.11 cm^2 total module area is the highest certified PCE of an OPV module >200 cm^2 to this date, and it thus constitutes a new world record, as further confirmed by the official "Champion Photovoltaic

Table 1. Photovoltaic key parameters of the 204-cm^2 PM6:Y6-C12:PC$_{61}$BM-based OPV module as measured in-house and obtained by certified measurements by Fraunhofer ISE (Freiburg, Germany)

Measurement	V_{OC} (V)	I_{SC} (Ma)	FF (%)	V_{MPP} (V)	I_{MPP} (mA)	P_{MPP} (W)	PCE (%) total area	PCE (%) active area
In-house	31.5	124.1	76.0	26.0	114.2	2.97	14.55	15.08
Certified	31.6 ± 0.13	125.3 ± 1.7	74.6 ± 0.4	26.12	113.0	2.952 ± 0.043	14.46 ± 0.21	14.98 ± 0.22

Module Efficiency Chart" by the National Renewable Energy Laboratory (NREL, Golden/USA).[12] Last but not least, notably, the previously reported high reproducibility (100% production yield and narrow PCE distribution)[14] also applies to the modules in this work, which is confirmed by the fact that actually three modules have been sent for certification, and all of them yielded similar certified PCE values (14.4% ± 0.1%).

Conclusions

We reported an OPV module with 14.5% certified PCE, which constitutes a new world record for OPV modules with areas >200 cm^2. Besides the quantified inevitable losses due to ITO resistance and GFF, hardly any difference in PCE is observed, compared with the >5,000 times smaller reference cells. This achievement was enabled by different FEM simulations that, on the one hand, analyzed and optimized the blade coating process to obtain homogeneous films on large areas and, on the other hand, provided the perfect module layout to minimize electrical and geometrical losses.

This surpasses the previous record (13.1% PCE by Waystech) by 11%, relatively, and reduces the efficiency gap between OPV record cells and modules from 32% to 24%.[1,12] Since this gap is found to be in the range of 10%–15% for all first- and second-generation PV technologies, this will also be a realistic target for emerging third-generation PV technologies, like OPVs, once they have reached their full performance potential.

EXPERIMENTAL PROCEDURES

Resource availability

Lead contact

Further information and requests for resources and materials should be directed to and will be fulfilled by the lead contact, Andreas Distler (andreas.distler@fau.de).

Materials availability

This study did not generate new unique materials.

Data and code availability

The datasets generated in this study are available from the lead contact on reasonable request.

Materials

Glass/ITO substrates with 11 Ω/sq were acquired from Liaoning Yike Precision New Energy Technology. The sol-gel ZnO precursor solution was prepared following the recipe by Baek et al.[24] Poly[(2,6-(4,8-bis(5-(2-ethylhexyl-3-fluoro)thiophen-2-yl)-benzo[1,2-b:4,5-b′]dithiophene))-alt-(5,5-(1′,3′-di-2-thienyl-5′,7′-bis(2-ethylhexyl) benzo[1′,2′-c:4′,5′-c′]dithiophene-4,8-dione)] (PBDB-T-2F, alias "PM6") and 2,2′-((2Z,2′Z)-((12,13-bis(2-butyloctyl)-3,9-diundecyl-12,13-dihydro-[1,2,5]thiadiazolo [3,4e]thieno[2″,3″:4′,5′]thieno[2′,3′:4,5]pyrrolo[3,2-g]thieno[2′,3′:4,5]thieno[3,2-b] indole-2,10-diyl)bis(methanylylidene))bis(5,6-difluoro-3-oxo-2,3-dihydro-1H-indene-2,1-diylidene))dimalononitrile (BTP-4F-C12, alias "Y6-C12") were synthesized at

Brilliant Matters. [6,6]-Phenyl-C61-butyric acid methyl ester ($PC_{61}BM$) was acquired from Nano-C.

PEDOT:F was synthesized according to the previously published recipe.[25] Silver (Ag) slugs for evaporation were purchased from Evochem.

Device fabrication

All devices fabricated in this work possess an inverted ("n-i-p") OPV architecture. The complete layer stack is glass/ITO/ZnO/PM6:Y6-C12:$PC_{61}BM$/PEDOT:F/Ag.

The coating steps are performed with a Zehntner ZAA 2300 blade coating device that was electrically modified by Automatic Research to enable pre-programming of time-dependent speed profiles, as described in more detail in Gumpert et al.[21] The laser patterning steps "P1", "P2a", "P2b", and "P3" are performed as reported previously.[14] For "P1", "P2a", and "P2b" a Spirit 1040-8 SHG laser from Spectra Physics (P_{max} = 6 W, λ = 520 nm, Yb:KYW) with 350 fs femtosecond pulse width in combination with a galvanometer scanner with f-theta lens and a focal length of 506 mm is used. "P3" is conducted by means of a Nanio Air laser by InnoLas Photonics (P_{max} = 10 W, λ = 532 nm, Nd:YVO4) with 20 ns pulse width in combination with the same galvanometer scanner.

The glass/ITO substrates are "P1" laser-patterned, wiped off with an isopropanol-soaked microfiber tissue, and finalized by a cleaning step in an industrial dishwasher. As shown in Figure S7, wiping the substrates manually right before the ETL coating (i.e., after the dishwasher) leads to inhomogeneities in the ZnO layer (rough surface in the shape of streaks at the starting positions of the wiping), which is why the cleaning order was reversed. In addition, right before coating the ETL, the substrate is flooded with isopropanol and blow-dried. The sol-gel ZnO precursor solution is filtered through a 0.45-μm polypropylene filter and subsequently coated with a doctor blade at 50°C in ambient air. Subsequently, the "P2a" laser patterning step is conducted, followed by annealing at 200°C for 30 min in ambient air. PM6, Y6-C12, and $PC_{61}BM$ (ratio: 1:1.2:0.24) are dissolved in o-xylene (total solid content: 22 mg/ml) and stirred at 80°C for 8 h. During blade coating of the active layer onto the ZnO at 60°C, the solution temperature is also reduced to 60°C. The PEDOT:F is deposited onto the active layer at 45°C. Subsequently, the devices are annealed at 140°C for 5 min under an inert atmosphere, followed by the "P2b" laser patterning step. Finally, 100 nm Ag is thermally evaporated, followed by the "P3" laser patterning step.

The large-area module is encapsulated using a top-glass cover and a UV-curable epoxy glue (DELO LP655). Finally, a self-adhesive anti-refection foil by Liaoning Yike Precision New Energy Technology (Film-H) is applied.

Characterization

I-V measurements of the solar cells and modules are performed with a class AAA solar simulator from LOT Quantum Design (LS0916 AAA) and a Keysight B2901A source measure unit (SMU) for cells and a Keithley 2450 SMU for modules. UV-vis spectra were recorded with a Shimadzu UV-1800 spectrometer.

Simulations

For the numerical modeling of the large-area blade coating processes, we performed CFD simulations using the platform COMSOL Multiphysics, which utilizes FEM to solve differential equations. Details about the creation of this model can be found in previous publications.[15,18] The electrical simulation of the large-area

OPV module as a function of cell number and applied external voltage is carried out using COMSOL's AC/DC module. The respective geometries and parameters are provided in the supplemental information.

SUPPLEMENTAL INFORMATION

Supplemental information can be found online at https://doi.org/10.1016/j.joule.2024.02.016.

ACKNOWLEDGMENTS

This work was financially supported by the Bavarian State Ministry of Science and the Arts (StMWK) via the Energy Campus Nürnberg (EnCN). The authors acknowledge funding from the European Union's Horizon 2020 Research and Innovation Program (H2020 Societal Challenges) under grant numbers 952911 (BOOSTER) and 101007084 (CITYSOLAR) and the German Federal Ministry for Economic Affairs and Climate Action via the ZIM project "OPV4IoT" (FKZ: 16KN098724). The authors further acknowledge funding from the Sino-German Center for Research Promotion (SGC) (Mobility Programme, GZ M-0160). Y.Z. acknowledges funding from the National Natural Science Foundation of China (grant number: 52273180).

AUTHOR CONTRIBUTIONS

Conceptualization, A.D.; methodology, J.L., and A.D.; investigation, R.B. and F.G.; resources, J.L., P.-O.M., V.V., Y.L., Y.Z., C.J.B., and H.-J.E.; writing – original draft, R.B. and A.D.; writing – review & editing, all co-authors; visualization, A.D.; supervision, J.L. and A.D.; project administration, A.D.; funding acquisition, J.L., Y.Z., C.J.B., H.-J.E., and A.D.

DECLARATION OF INTERESTS

The authors declare no competing interests.

Received: January 19, 2024
Revised: February 6, 2024
Accepted: February 16, 2024
Published: March 6, 2024

REFERENCES

1. NREL. Best Research-Cell Efficiency Chart. https://www.nrel.gov/pv/cell-efficiency.html.

2. Zhang, G., Lin, F.R., Qi, F., Heumüller, T., Distler, A., Egelhaaf, H.-J., Li, N., Chow, P.C.Y., Brabec, C.J., Jen, A.K.-Y., and Yip, H.-L. (2022). Renewed Prospects for Organic Photovoltaics. Chem. Rev. *122*, 14180–14274.

3. Zhang, B., Yang, F., and Li, Y. (2023). Recent Progress in Large-Area Organic Solar Cells. Small Sci. *3*, 2300004.

4. Wachsmuth, J., Distler, A., Liu, C., Heumüller, T., Liu, Y., Aitchison, C.M., Hauser, A., Rossier, M., Robitaille, A., Llobel, M.-A., et al. (2023). Fully Printed and Industrially Scalable Semitransparent Organic Photovoltaic Modules: Navigating through Material and Processing Constraints. Sol. RRL *7*, 2300602.

5. Wang, G., Zhang, J., Yang, C., Wang, Y., Xing, Y., Adil, M.A., Yang, Y., Tian, L., Su, M., Shang, W., et al. (2020). Synergistic Optimization Enables Large-Area Flexible Organic Solar Cells to Maintain over 98% PCE of the Small-Area Rigid Devices. Adv. Mater. *32*, e2005153.

6. Sun, R., Wang, T., Yang, X., Wu, Y., Wang, Y., Wu, Q., Zhang, M., Brabec, C.J., Li, Y., and Min, J. (2022). High-speed sequential deposition of photoactive layers for organic solar cell manufacturing. Nat. Energy *7*, 1087–1099.

7. Dong, S., Jia, T., Zhang, K., Jing, J., and Huang, F. (2020). Single-Component Non-halogen Solvent-Processed High-Performance Organic Solar Cell Module with Efficiency over 14%. Joule *4*, 2004–2016.

8. Chen, H., Zhang, R., Chen, X., Zeng, G., Kobera, L., Abbrent, S., Zhang, B., Chen, W., Xu, G., Oh, J., et al. (2021). A guest-assisted molecular-organization approach for >17% efficiency organic solar cells using environmentally friendly solvents. Nat. Energy *6*, 1045–1053.

9. Zhang, B., Yang, F., Chen, S., Chen, H., Zeng, G., Shen, Y., Li, Y., and Li, Y. (2022). Fluid Mechanics Inspired Sequential Blade-Coating for High-Performance Large-Area Organic Solar Modules. Adv. Funct. Mater. *32*, 2202011.

10. Jia, Z., Chen, Z., Chen, X., Yao, J., Yan, B., Sheng, R., Zhu, H., and Yang, Y. (2021). 19.34 cm^2 large-area quaternary organic photovoltaic module with 12.36% certified efficiency. Photonics Res. *9*, 324–330.

11. Faisst, J., Jiang, E., Bogati, S., Pap, L., Zimmermann, B., Kroyer, T., Würfel, U., and List, M. (2023). Organic Solar Cell with an Active Area > 1 cm^2 Achieving 15.8% Certified Efficiency using Optimized VIS-NIR Antireflection Coating. Sol. RRL *7*, 2300663.

12. NREL. Champion Photovoltaic Module Efficiency Chart. https://www.nrel.gov/pv/module-efficiency.html.

13. Rakocevic, L., Schöpe, G., Turan, B., Genoe, J., Aernouts, T., Haas, S., Gehlhaar, R., and Poortmans, J. (2020). Perovskite modules with 99% geometrical fill factor using point contact

interconnections design. Progress in Photovoltaics *28*, 1120–1127.

14. Distler, A., Brabec, C.J., and Egelhaaf, H.-J. (2021). Organic photovoltaic modules with new world record efficiencies. Progress in Photovoltaics *29*, 24–31.

15. Hong, L., Yao, H., Wu, Z., Cui, Y., Zhang, T., Xu, Y., Yu, R., Liao, Q., Gao, B., Xian, K., et al. (2019). Eco-Compatible Solvent-Processed Organic Photovoltaic Cells with Over 16% Efficiency. Adv. Mater. *31*, 1903441.

16. Li, P., Hoff, A., Gasonoo, A., Niazi, M.R., Nazari, M., and Welch, G.C. (2023). Layer-by-Layer Processed Organic Photovoltaic Cells Using Slot-Die-Coating Methods and Non-halogenated Solvents under Ambient Conditions with PCE of 10%. Adv. Mater. Interfaces *10*, 2202156.

17. Pan, M.-A., Lau, T.-K., Tang, Y., Wu, Y.-C., Liu, T., Li, K., Chen, M.-C., Lu, X., Ma, W., and Zhan, C. (2019). 16.7%-efficiency ternary blended organic photovoltaic cells with PCBM as the acceptor additive to increase the open-circuit voltage and phase purity. J. Mater. Chem. A *7*, 20713–20722.

18. Gumpert, F., Janßen, A., Brabec, C.J., Egelhaaf, H.-J., Lohbreier, J., and Distler, A. (2023). Predicting layer thicknesses by numerical simulation for meniscus-guided coating of organic photovoltaics. Eng. Appl. Comp. Fluid Mech. *17*, 2242455.

19. Nickel, F., Sprau, C., Klein, M.F.G., Kapetana, P., Christ, N., Liu, X., Klinkhammer, S., Lemmer, U., and Colsmann, A. (2012). Spatial mapping of photocurrents in organic solar cells comprising wedge-shaped absorber layers for an efficient material screening. Sol. Energy Mater. Sol. Cells *104*, 18–22.

20. Tsai, P.-T., Yu, K.-C., Chang, C.-J., Horng, S.-F., and Meng, H.-F. (2015). Large-area organic solar cells by accelerated blade coating. Org. Electron. *22*, 166–172.

21. Gumpert, F., Janßen, A., Basu, R., Brabec, C.J., Egelhaaf, H.-J., Lohbreier, J., and Distler, A. (2024). On the theoretical framework for meniscus-guided manufacturing of large-area OPV modules. Preprint at arXiv.

22. Würfel, U., Herterich, J., List, M., Faisst, J., Bhuyian, M.F.M., Schleiermacher, H.-F., Knupfer, K.T., and Zimmermann, B. (2021). A 1 cm^2 Organic Solar Cell with 15.2% Certified Efficiency: Detailed Characterization and Identification of Optimization Potential. Sol. RRL *5*, 2000802.

23. Lucera, L., Kubis, P., Fecher, F.W., Bronnbauer, C., Turbiez, M., Forberich, K., Ameri, T., Egelhaaf, H.-J., and Brabec, C.J. (2015). Guidelines for Closing the Efficiency Gap between Hero Solar Cells and Roll-To-Roll Printed Modules. Energy Technol. *3*, 373–384.

24. Baek, S.-W., Jun, S., Kim, B., Proppe, A.H., Ouellette, O., Voznyy, O., Kim, C., Kim, J., Walters, G., Song, J.H., et al. (2019). Efficient hybrid colloidal quantum dot/organic solar cells mediated by near-infrared sensitizing small molecules. Nat. Energy *4*, 969–976.

25. Jiang, Y., Dong, X., Sun, L., Liu, T., Qin, F., Xie, C., Jiang, P., Hu, L., Lu, X., Zhou, X., et al. (2022). An alcohol-dispersed conducting polymer complex for fully printable organic solar cells with improved stability. Nat. Energy *7*, 352–359.